SAND2021-13778R

Sandia National Laboratories

Operated for the U.S. Department of Energy by

National Technology and Engineering Solutions of Sandia

Albuquerque, New Mexico 87185

date: October 29, 2021

to: Distribution

from: C. Vignes (1558), B. Lester (1558)

reviewed: W. Scherzinger (1558)

subject: Inclusion of tearing parameter failure capabilities in modular failure

Abstract

The tearing parameter criterion and failure propagation method currently used in the multilinear elastic-plastic constitutive model was added as an option to modular failure capabilities. Currently, this implementation is only available to the J_2 plasticity model due to the formulation of the failure propagation approach. The implementation was verified against analytical solutions for both a uni-axial tension and a pure shear boundary-value problem. Possible improvements to, and necessary generalizations of, the failure method to extend it as a modular option for all plasticity models are highlighted.

Sandia National Laboratories is a multi-mission laboratory managed and operated by National Technology and Engineering Solutions of Sandia, LLC., a wholly owned subsidiary of Honeywell International, Inc., for the U.S. Department of Energy's National Nuclear Security Administration under contract DE-NA0003525.

Exceptional Service in the National Interest

Sandia National Laboratories is a multimission laboratory managed and operated by National Technology & Engineering Solutions of Sandia, LLC, a wholly owned subsidiary of Honeywell International Inc., for the U.S. Department of Energy's National Nuclear Security Administration under contract DE-NA0003525.

1 Introduction

A recent focus with modular plasticity models in the Library of Advanced Materials for Engineering (LAMÉ) [1] has been the expansion of capabilities to include failure models. A failure model consists of both a failure criterion and a failure propagation method. Current work has included adding a variety of modular failure criterion [2], both continuum-level and microstructurally motivated, such as the BCJ failure criterion [3], as well as initial efforts to expand available failure propagation methods beyond element death.

Failure methods including material softening via damage are currently limited in LAMÉ. Two softening approaches may be found in different LAMÉ models. The first is the critical crack opening strain, linear softening method embedded in the multilinear elastic-plastic (MLEP) material model which uses the tearing parameter as a failure criterion [4]. The second is the class of microstructurally motivated softening models (e.g., BCJ). This memo details the first approach; that is, the modularization of the critical crack opening strain, linear softening failure method from the MLEP model and its application to the J_2 plasticity model.

2 Theory

2.1 Tearing parameter

For the modular failure criterion, a tearing parameter damage variable d is implemented [2] as a normalization of the modified tearing parameter t_p in Wellman [4] and defined as

$$d = \frac{t_p}{t_p^{crit}} = \frac{1}{t_p^{crit}} \int_0^{\bar{\varepsilon}^p} \left\langle \frac{2\sigma_{max}}{3(\sigma_{max} - p)} \right\rangle^m d\hat{\bar{\varepsilon}}^p. \tag{1}$$

Here, σ_{max} is the maximum principal stress and pressure $p = \frac{1}{3}\text{tr}(\boldsymbol{\sigma})$ is the trace of the Cauchy stress tensor $\boldsymbol{\sigma}$. Also, $\bar{\varepsilon}^p$ is the equivalent plastic strain and $\langle \cdot \rangle$ are Macaulay brackets. The damage variable has two model parameters; m, a fitting exponent, and t_p^{crit}, the critical tearing parameter. During loading, the damage value increases from $d = 0$ in the initial state to the critical damage value $d = 1$. For uniaxial tension, the integrand in the damage variable is one and the tearing parameter is equal to the equivalent plastic strain, $t_p = \bar{\varepsilon}^p$.

2.2 Failure propagation

For the failure method in Wellman [4], failure initiates at the critical damage value (Figure 1). Prior to failure initiation, the underlying plasticity model is unaltered; the material response is linear elastic until yield (ε_y) and then elastic-plastic until critical damage (ε_d). Once the damage (tearing parameter) criterion is satisfied, stress decays linearly to zero over a critical crack opening strain of magnitude ε_{ccos}, after which the stress remains zero at failure (ε_f). The Macaulay brackets ensure the damage variable (1) is non-zero, and failure initiates only for tensile stress states. This failure method will be referred to as the critical crack opening strain, linear softening method.

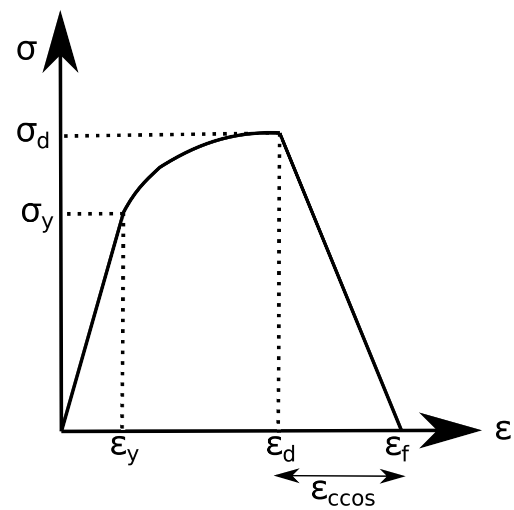

Figure 1. Stress-strain curve for plasticity model with failure.

The damage value is computed at every converged plastic state. At the transition between plasticity and failure, the stress state may cause the damage value to exceed the critical damage value ($d = 1$). For this load step, the strain is partitioned into the plastic strain required to satisfy the damage criterion and the excess strain, considered crack opening strain, used to decay the stresses. The stress state is scaled back to the critical damage stress $\boldsymbol{\sigma}_d$ and this stress is then linearly decayed.

At the transition step, let $\boldsymbol{\sigma}_n$ be the converged stress state at the end of the previous timestep and $\boldsymbol{\sigma}_{n+1}$ be the stress state at the current timestep without failure. However, for $\boldsymbol{\sigma}_{n+1}$, the critical damage value is exceeded, $d_{n+1} > 1$, so the critical damage stress $\boldsymbol{\sigma}_d$ is the stress state without failure scaled back to the stress state at the critical damage value, namely,

$$\boldsymbol{\sigma}_d = \boldsymbol{\sigma}_n + (\boldsymbol{\sigma}_{n+1} - \boldsymbol{\sigma}_n)\left(\frac{1 - d_n}{d_{n+1} - d_n}\right). \tag{2}$$

Similarly, the strain increment for the transition step is partitioned between plastic strain and crack opening strain. The direction of crack opening, denoted by the normal vector $\boldsymbol{n}_d$ is assumed to be aligned with the maximum principal stress during the transition step and is fixed once the crack is initiated. The crack opening strain increment is

$$(\varepsilon_{cos})_{n+1} = (\varepsilon_{cos})_n + \max\left\{0, \gamma(\boldsymbol{n}_d \cdot \dot{\boldsymbol{\varepsilon}}_{n+1}\boldsymbol{n}_d)\Delta t\right\}, \tag{3}$$

where

$$\gamma = \begin{cases} \frac{d_{n+1}-1}{d_{n+1}-d_n} & \text{for the transition step,} \\ 1 & \text{afterwards.} \end{cases} \tag{4}$$

The maximum term in (3) prevents damage healing. The decay factor is given as

$$\alpha_{n+1} = \max\left\{0, \frac{\varepsilon_{ccos} - (\varepsilon_{cos})_{n+1}}{\varepsilon_{ccos}}\right\}. \tag{5}$$

Finally, stress is decayed by decreasing the maximum yield stress, $\bar{\sigma}_d = \phi(\boldsymbol{\sigma}_d)$ (or equivalently the maximum radius $r_d = \frac{2}{3}\bar{\sigma}_d$), as

$$\bar{\sigma}(\bar{\varepsilon}^p)_{n+1} = \alpha_{n+1} \cdot \bar{\sigma}_d, \tag{6}$$

and radially returning to this reduced yield stress. Here, ϕ is the effective stress and $\bar{\sigma}$ the hardening function in the yield surface $f(\boldsymbol{\sigma}, \boldsymbol{\alpha}) = \phi(\boldsymbol{\sigma}, \boldsymbol{\alpha}) - \bar{\sigma}(\bar{\varepsilon}^p)$ where $\boldsymbol{\alpha}$ is the back stress tensor. Note, the use of a radial return constrains the failure method to an isotropic yield surface and limits the plasticity model to J_2 formulations. In the current implementation, a von Mises effective stress is used. The algorithmic implementation is outlined in Box 1 (where $\boldsymbol{s}$ is the deviatoric stress tensor).

Wellman [4] notes that for cases of complete constraint, this technique will decay the deviatoric stress to zero, but a hydrostatic stress may remain. In such cases, a change in loading that would create a deviatoric stress causes simulations to become unstable since a deviatoric stress can no longer be sustained. To address these cases, the pressure is checked against the maximum pressure, $p_d = \frac{1}{3}\mathrm{tr}(\boldsymbol{\sigma}_d)$, and, if necessary, further decayed such that

$$p_{n+1} \leq \alpha_{n+1} \cdot p_d. \tag{7}$$

At the conclusion of the transition step, the damage value is set to the critical damage value, $d_{n+1} = 1$, and all subsequent damage values are also fixed at this value.

Wellman [4] also noted that the critical crack opening strain ε_{ccos} parameter is related to the energy dissipation in an element. Careful selection of the critical crack opening strain value can be important in reducing mesh dependency; see Wellman [4] for a detailed discussion and guidance.

3 Algorithm

The failure propagation theory in Section 2.2 describes the process applicable to any finite element. However, for multi-element simulations, Wellman [4] discusses convergence issues with the direct implementation of this technique in the constitutive model and the resolution of these issues with a multilevel solver algorithm. To assist in the coupling of the constitutive model to the multilevel solver, a set of five crack failure flags is defined for each element as follows:

(1) Crack flag = 0.
The damage criterion, $d_{n+1} \geq 1$, has not been satisfied. Crack initiation has not occurred in the element. Material response is the underlying plasticity model.

(2) Crack flag = 1.
The damage criterion, $d_{n+1} \geq 1$, has been satisfied for the element.

(3) Crack flag = 2.
The element exceeded the damage criterion the most out of all elements marked with crack flag = 1. Mark as a transition step and use partitioned stress decay. See Box 1.

(4) Crack flag = 3.
The element is in failure. Material response is stress decay. See Box 1.

(5) Crack flag = 4.
The element has failed. Stress is identically zero.

(1) Check if transition step and set parameters:

`If` crack flag = 2

$$\boldsymbol{\sigma}_d = \boldsymbol{\sigma}_n + (\boldsymbol{\sigma}_{n+1} - \boldsymbol{\sigma}_n)\left(\frac{1-d_n}{d_{n+1}-d_n}\right)$$

$$r_d = \frac{2}{3}\phi(\boldsymbol{\sigma}_d), \quad p_d = \frac{1}{3}\mathrm{tr}(\boldsymbol{\sigma}_d)$$

$$\gamma = \frac{d_{n+1}-1}{d_{n+1}-d_n}$$

`else` (crack flag = 3):

$$\gamma = 1$$

`end`

(2) Strain increment magnitude in crack opening direction:

$$(\varepsilon_{cos})_{n+1} = (\varepsilon_{cos})_n + \max\{0, \gamma(\boldsymbol{n}_d \cdot \Delta\dot{\boldsymbol{\varepsilon}}_{n+1}\boldsymbol{n}_d)\Delta t\}$$

(3) Critical crack opening strain check:

`If` $(\varepsilon_{cos})_{n+1} > \varepsilon_{ccos}$

$$\boldsymbol{\sigma}_{n+1} = \mathbf{0}$$

`else`:

$$\alpha_{n+1} = \frac{\varepsilon_{ccos} - (\varepsilon_{cos})_{n+1}}{\varepsilon_{ccos}}$$

$$r_{n+1} = \alpha_{n+1} r_d$$

$$\boldsymbol{\alpha}_{n+1} = \mathbf{0}$$

$$\boldsymbol{\sigma}^{TR}_{n+1} = \boldsymbol{\sigma}_n + 2G(\Delta\dot{\boldsymbol{\varepsilon}}^{dev}_{n+1})\Delta t + K(\Delta\dot{\varepsilon}^{vol}_{n+1})\Delta t\boldsymbol{I}$$

`If` $\|\boldsymbol{s}^{TR}_{n+1}\| > r_{n+1}$

$$\boldsymbol{\sigma}_{n+1} = \boldsymbol{\sigma}^{TR}_{n+1} - (\|\boldsymbol{s}^{TR}_{n+1}\| - r_{n+1})\boldsymbol{N}^{TR}_{n+1} = \boldsymbol{\sigma}^{TR}_{n+1} - \left(1 - \frac{r_{n+1}}{\|\boldsymbol{s}^{TR}_{n+1}\|}\right)\boldsymbol{s}^{TR}_{n+1}$$

`else`:

$$\boldsymbol{\sigma}_{n+1} = \boldsymbol{\sigma}^{TR}_{n+1}$$

`end`

$$p_{n+1} = \frac{1}{3}\mathrm{tr}(\boldsymbol{\sigma}_{\mathrm{n+1}})$$

`If` $p_{n+1} > \alpha_{n+1} \cdot p_d$ `and` $\alpha_{n+1} > tol_\alpha$

$$\boldsymbol{s}_{n+1} = \boldsymbol{\sigma}_{n+1} - p_{n+1}\boldsymbol{I}$$

$$(\sigma_{ii})_{n+1} = (s_{ii})_{n+1} + p_{n+1} \cdot \alpha_{n+1}, \quad ii = 11, 22, \text{and } 33$$

`end`

`end`

Box 1 : Failure algorithm for transition step (crack flag 2) and stress decay (crack flag 3).

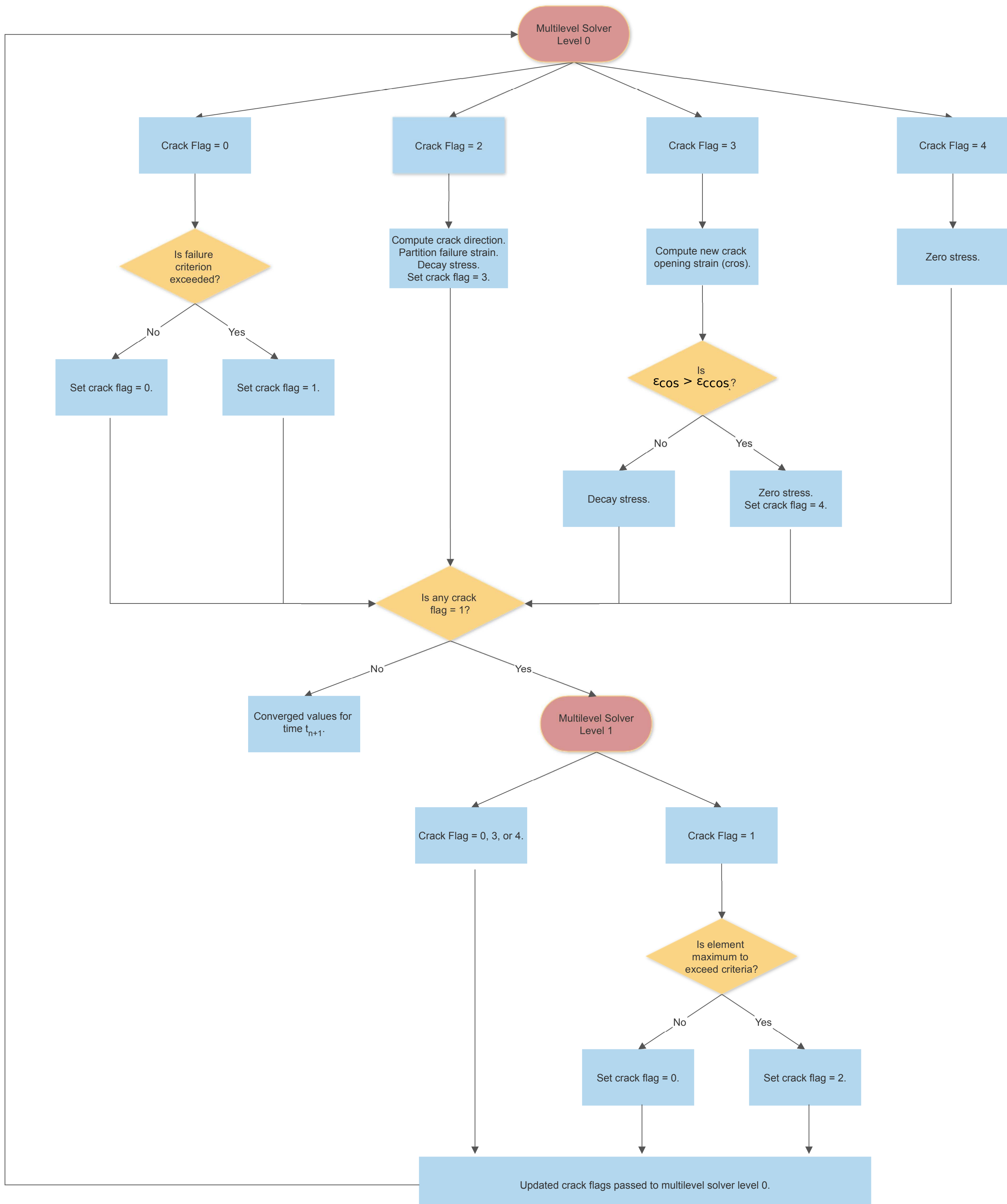

Figure 2. Failure flowchart.

Figure 2 is a failure flowchart for the multilevel solver with crack flags; the multilevel solution algorithm is also described in Box 2. The plasticity response and stress decay response are local to the constitutive model (multilevel solver Level 0) while the inter-element damage criterion comparison is nonlocal and managed outside the constitutive model by the solver (multilevel solver Level 1).

(1) Start new load step.

(2) Multilevel solver: Level 0

   (a) Converge solution.

   (b) Mark undamaged elements (crack flag = 0) which exceed the damage criterion by advancing crack flag = 1.

(3) Multilevel solver: Level 1

   (a) Do any elements exceed the damage criterion (crack flag = 1)?
   No – go to (4)
   Yes – continue

   (b) From all possible elements undergoing the transition step from plasticity to failure (crack flag = 1), select the element most exceeding the damage criterion and set crack flag = 2.

   (c) For remaining elements with crack flag = 1, reset crack flag = 0.

   (d) Return to (2)

(4) Multilevel solver: Level 0

   (a) For all elements which completed the transition step (crack flag = 2), advance to the decay regime by setting crack flag = 3.

   (b) For all elements that have decayed to zero stress, advance crack flag = 4.

(5) Update state variable and go to (1).

Box 2 : Multilevel solution algorithm for failure.

At the start of a new load step, the multilevel solver begins in Level 0. All elements are either undamaged (crack flag 0), in the stress decay failure regime (crack flag 3), or failed with the stress identically zero (crack flag 4). For this set of crack flags, the first solution iteration is converged; undamaged elements (crack flag 0) respond according to the underlying plasticity model, stress decay elements (crack flag 3) linearly decay the stress according to the failure propagation technique described in Section 2.2 and Box 1, and failed elements (crack flag 4) remain unchanged with zero stress. After the first solution iteration, the undamaged elements (crack flag 0) are checked against the damage criterion and all that exceed the criterion are marked with crack flag 1.

After the first solution iteration, control is passed to multilevel solver Level 1. Here, the solver checks if any element is marked as exceeding the damage criterion (crack flag 1). If not, the first solution iteration is the converged solution, control is passed back to multilevel solver Level 0 to update state variables, and the next load step is initiated or the simulation completed. However, if elements are marked with crack flag 1, the Level 1 solver identifies the undamaged element which exceeded the damage criterion the most and marks this element (setting crack flag 2) for a transition step from plasticity to failure. All remaining elements that exceeded the damage criterion (crack flag 1) are reset to undamaged elements (crack flag 0). Solution control is returned to the Level 0 solver and a second solution iteration is converged. During this iteration, the transition element (crack flag 2) response is part plasticity and part stress decay according to the failure propagation technique described in Section 2.2 and Box 1. Again, the undamaged elements (crack flag 0) are checked against the damage criterion and all that exceed the criterion are marked with crack flag 1. This set of elements is possibly different than the set in the previous solution iteration as the transitioned element may alter the stress state in the neighboring elements.

Solution control iterates between the Level 0 solver and Level 1 solver as one element completes the transition step per iteration. When no more undamaged elements exceed the damage criterion at the end of a multilevel solution iteration, the transition elements (crack flag 2) are advanced to the stress decay regime (crack flag 3), fully decayed elements with zero stress are marked as failed (crack flag 4), state variables are updated, and the next load step is initiated or the simulation completed.

4 Verification

The tearing parameter criterion and failure propagation method was implemented as a modular failure option for the J_2 plasticity model. The modular failure implementation is verified for a uniaxial tension test and pure shear test.

4.1 Uniaxial tension

The verification boundary-value problem is uniaxial tension of a unit cube. Three faces of a unit cube intersecting at the origin are fixed in their normal directions. A constant logarithmic strain rate ramp load is applied to the cube in the x_1-direction by specifying the applied displacement in this direction as

$$u_1 = (e^{\varepsilon_L\left(\frac{t}{t_L}\right)} - 1)X_1 \tag{8}$$

where ε_L is the loading strain and t_L is the ramp loading time (Figure 3). Here, the logarithmic axial strain is $\varepsilon_L = 0.05$ and $t_L = 1$ s. The logarithmic strain in the applied displacement direction is

$$\varepsilon_{11} = \varepsilon_L\left(\frac{t}{t_L}\right). \tag{9}$$

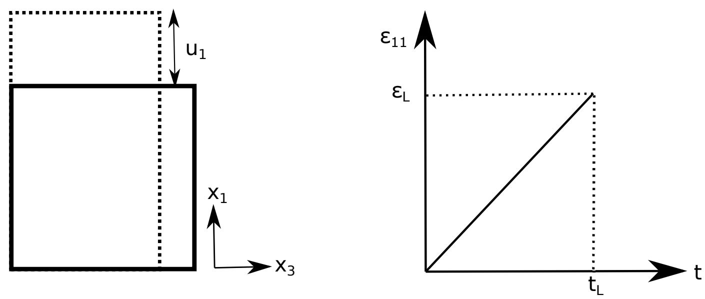

Figure 3. Applied loading and strain history for uniaxial tension.

The material parameters used are shown in Table 1. For the plasticity model, a linear hardening rule is assumed and given by

$$\bar{\sigma}(\bar{\varepsilon}^p) = \sigma_y + H'\bar{\varepsilon}^p, \tag{10}$$

where σ_y is the yield stress and H' the hardening modulus.

E	70 GPa
ν	0.25 MPa

HARDENING MODEL	LINEAR
FAILURE MODEL	TP_CCOS_LINEAR_SOFTENING

σ_y	200 MPa
H'	500 MPa

t_p^{crit}	0.04
ε_{ccos}	0.005
m	4.0

Table 1. The material properties for the J_2 plasticity model with tearing parameter failure.

For uniaxial tension, the analytical Cauchy stress in the loading direction is

$$\sigma_{11}(t) = \begin{cases} E\varepsilon_{11} & \text{for } \varepsilon_{11} \le \varepsilon_y \\ \left(\frac{E}{E+H'}\right)(\sigma_y + H'\varepsilon_{11}) & \text{for } \varepsilon_y < \varepsilon_{11} \le \varepsilon_d \\ \left(\frac{\varepsilon_{ccos}-(\varepsilon_{11}-\varepsilon_d)}{\varepsilon_{ccos}}\right)(\sigma_y + H' t_p^{crit}) & \text{for } \varepsilon_d < \varepsilon_{11} \le \varepsilon_f \\ 0 & \text{for } \varepsilon_f < \varepsilon_{11} \le \varepsilon_L \end{cases} \tag{11}$$

where

$$\varepsilon_y = \frac{\sigma_y}{E}, \qquad \varepsilon_d = \varepsilon_y + \left(1 + \frac{H'}{E}\right) t_p^{crit}, \qquad \varepsilon_f = \varepsilon_d + \varepsilon_{ccos}. \tag{12}$$

For uniaxial tension, the maximum principal stress $\sigma_{max} = \sigma_{11}$ and the pressure $p = \frac{1}{3}\sigma_{11}$. With these values and the prescribed monotonic loading, the Macaulay bracket term in the tearing parameter damage variable (1) is identically one and the integral term reduces to the equivalent plastic strain. The damage variable d is then given by

$$d = \frac{\bar{\varepsilon}^p}{t_p^{crit}} = \begin{cases} 0 & \text{for } \varepsilon_{11} \leq \varepsilon_y \\ \frac{E\varepsilon_{11}-\sigma_y}{(E+H')t_p^{crit}} & \text{for } \varepsilon_y < \varepsilon_{11} \leq \varepsilon_d \\ 1 & \text{for } \varepsilon_{11} > \varepsilon_d \end{cases}. \tag{13}$$

The yield surface radius is $r = \sqrt{2/3}\sigma$, except prior to yielding when it is $r = \sqrt{2/3}\sigma_y$, or

$$r = \sqrt{\frac{2}{3}} \begin{cases} \sigma_y & \text{for } \varepsilon_{11} \leq \varepsilon_y \\ \left(\frac{E}{E+H'}\right)(\sigma_y + H'\varepsilon_{11}) & \text{for } \varepsilon_y < \varepsilon_{11} \leq \varepsilon_d \\ \left(\frac{\varepsilon_{ccos}-(\varepsilon_{11}-\varepsilon_d)}{\varepsilon_{ccos}}\right)(\sigma_y + H' t_p^{crit}) & \text{for } \varepsilon_d < \varepsilon_{11} \leq \varepsilon_f \\ 0 & \text{for } \varepsilon_f < \varepsilon_{11} \leq \varepsilon_L \end{cases} \tag{14}$$

The results of the analysis are shown in Figure 4 and Figure 5.

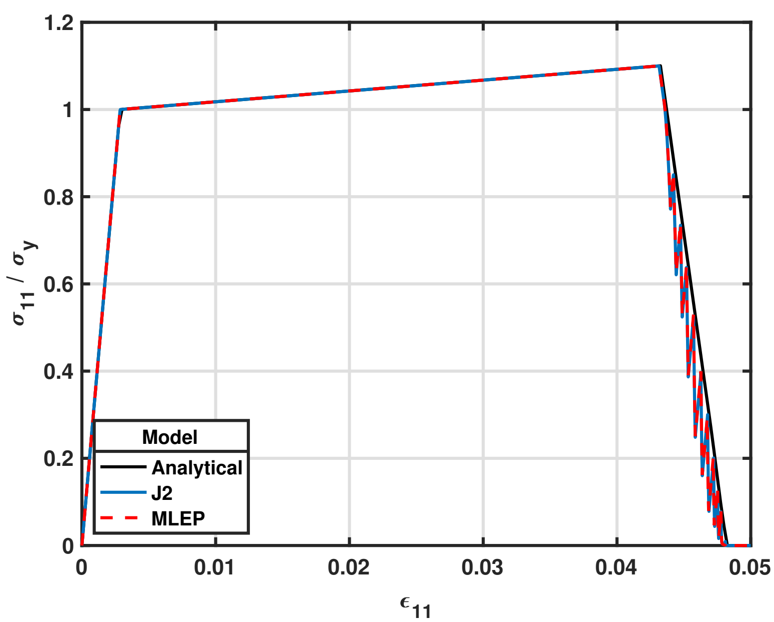

Figure 4. Stress-strain response for uniaxial tension.

Both the damage variable and radius match the analytical solutions well for the J_2 plasticity model with modular failure and the MLEP model. However, the axial stress response does not match the analytical solution during the stress decay phase for either the J_2 model implementation or the MLEP model. Instead of a linear decay of the axial stress to zero, the models exhibit oscillations.

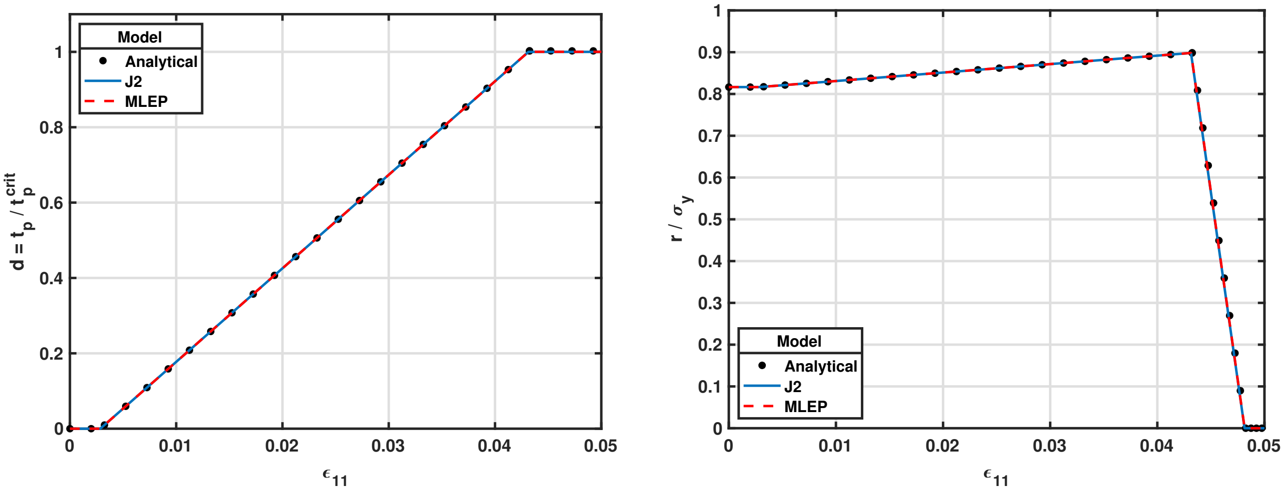

Figure 5. The (a) tearing parameter damage variable, and (b) yield surface radius for uniaxial tension.

First, the stress is over-decayed and then the stress elastically reloads to the analytical decay line before repeating the process. This oscillatory behavior is attributed to the additional hydrostatic stress check (7) and pressure decay technique noted by Wellman [4] as necessary for stability in constrained boundary-value problems.

From the algorithmic implementation of the failure method, Box 1, the last If − end block (copied in Box 3 (1)) in the critical crack opening strain check implements the pressure decay. Pressure decay only occurs if the condition $p_{n+1} > \alpha_{n+1} \cdot p_d$ is satisfied. This conditional check leads to a discrete pressure decay and the oscillations observed in the uniaxial tension problem.

(1) Discrete pressure decay:

If $p_{n+1} > \alpha_{n+1} \cdot p_d$ and $\alpha_{n+1} > tol_\alpha$

$$\boldsymbol{s}_{n+1} = \boldsymbol{\sigma}_{n+1} - p_{n+1}\boldsymbol{I}$$
$$(\sigma_{11})_{n+1} = (s_{11})_{n+1} + p_{n+1} \cdot \alpha_{n+1}$$
$$(\sigma_{22})_{n+1} = (s_{22})_{n+1} + p_{n+1} \cdot \alpha_{n+1}$$
$$(\sigma_{33})_{n+1} = (s_{33})_{n+1} + p_{n+1} \cdot \alpha_{n+1}$$

end

(2) Continuous pressure decay:

$$\boldsymbol{s}_{n+1} = \boldsymbol{\sigma}_{n+1} - p_{n+1}\boldsymbol{I}$$
$$(\sigma_{11})_{n+1} = (s_{11})_{n+1} + p_{n+1} \cdot \alpha_{n+1}$$
$$(\sigma_{22})_{n+1} = (s_{22})_{n+1} + p_{n+1} \cdot \alpha_{n+1}$$
$$(\sigma_{33})_{n+1} = (s_{33})_{n+1} + p_{n+1} \cdot \alpha_{n+1}$$

Box 3 : Discrete pressure decay and continuous pressure decay algorithms.

If this conditional check were removed, the discrete pressure decay algorithm, Box 3 (1), would become the continuous pressure decay algorithm, Box 3 (2). For continuous pressure decay, the pressure is always decayed. Figure 6 compares the axial stress responses for uniaxial tension with no pressure decay, the discrete pressure decay, and the continuous pressure decay. If the pressure decay algorithm is removed, the model solution matches the analytical solution. For continuous pressure decay, the decay oscillations are removed; however, the error in the model solution increases as the stress decay phase advances.

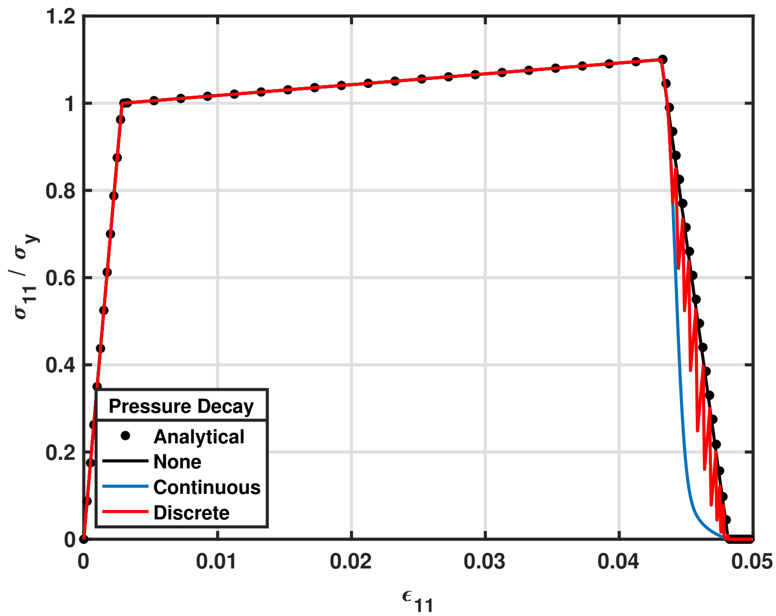

Figure 6. Stress-strain responses for uniaxial tension with different pressure decay techniques.

For the uniaxial tension boundary-value problem, the pressure decay algorithm introduced errors into the model solution; the model solution without added pressure decay was exact. More analysis is required, in particular a representative problem with stability issues, to determine the balance between incurring these errors and the stability of the solution. Pressure decay is an area for potential model improvements.

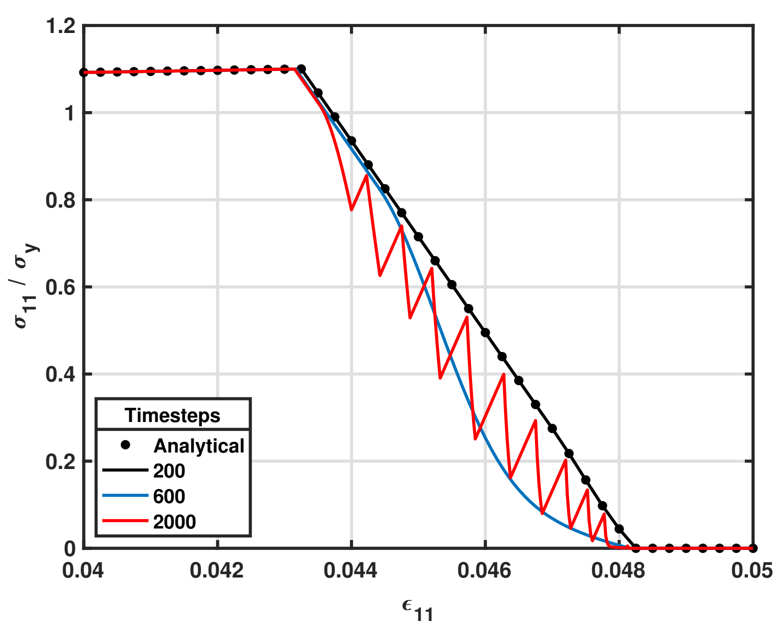

Figure 7. Stress-strain responses with discrete pressure decay for different timesteps.

Additionally, the discrete pressure decay currently implemented in both the J_2 plasticity model with modular failure and the MLEP model has timestep sensitivity. Figure 7 shows the stress decay portion of the axial stress-strain response with different timesteps. For large timesteps, the model solution converges to the analytical solution. As the timestep size is decreased, the stress decay becomes nonlinear and finally oscillatory.

4.2 Pure shear

A second verification boundary-value problem is pure shear of a unit cube. The faces with x_3-normals are fixed in the normal directions. A constant logarithmic strain rate ramp load (Figure 8) is applied to the cube in the $(x_1 x_2)$-plane by specifying the applied displacement as

$$u_1 = \frac{1}{2}\left(e^{\varepsilon_L\left(\frac{t}{t_L}\right)} + e^{-\varepsilon_L\left(\frac{t}{t_L}\right)} - 2\right)X_1 + \frac{1}{2}\left(e^{\varepsilon_L\left(\frac{t}{t_L}\right)} - e^{-\varepsilon_L\left(\frac{t}{t_L}\right)}\right)X_2 \tag{15}$$

$$u_2 = \frac{1}{2}\left(e^{\varepsilon_L\left(\frac{t}{t_L}\right)} - e^{-\varepsilon_L\left(\frac{t}{t_L}\right)}\right)X_1 + \frac{1}{2}\left(e^{\varepsilon_L\left(\frac{t}{t_L}\right)} + e^{-\varepsilon_L\left(\frac{t}{t_L}\right)} - 2\right)X_2. \tag{16}$$

Here, the loading strain is $\varepsilon_L = 0.025$ and $t_L = 1$ s. The shear strain is

$$\epsilon_{12} = \varepsilon_L\left(\frac{t}{t_L}\right) \tag{17}$$

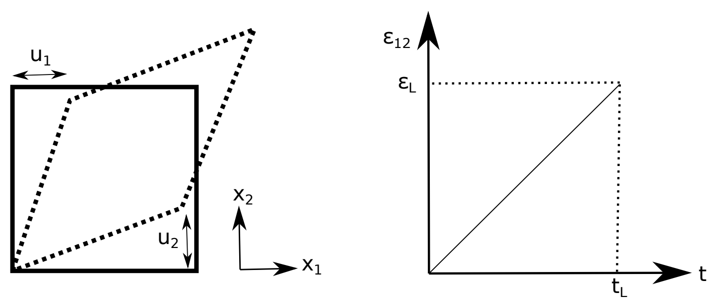

Figure 8. Applied loading and strain history for pure shear.

The material parameters used are the same as in Table 1 with the exception of $t_p^{crit} = 0.004$.

For pure shear, with shear modulus G, the analytical Cauchy stress in the shear plane is

$$\sigma_{12}(t) = \begin{cases} 2G\varepsilon_{12} & \text{for } \varepsilon_{12} \le \varepsilon_y \\ \left(\frac{1}{3G+2H'}\right)\left[\left(\frac{3G+H'}{\sqrt{3}}\right)\sigma_y + 2GH'\varepsilon_{12}\right] & \text{for } \varepsilon_y < \varepsilon_{12} \le \varepsilon_d \\ \left(\frac{\varepsilon_{ccos}-(\varepsilon_{12}-\varepsilon_d)}{\varepsilon_{ccos}}\right)\left(\frac{\sigma_y}{\sqrt{3}} + \frac{H'}{\sqrt{3}}\left(\frac{3}{2}\right)^4 t_p^{crit}\right) & \text{for } \varepsilon_d < \varepsilon_{12} \le \varepsilon_f \\ 0 & \text{for } \varepsilon_f < \varepsilon_{12} \le \varepsilon_L \end{cases} \tag{18}$$

where

$$\varepsilon_y = \frac{\sigma_y}{2\sqrt{3}G}, \qquad \varepsilon_d = \varepsilon_y + \left(\frac{3G+2H'}{2\sqrt{3}G}\right)\left(\frac{3}{2}\right)^4 t_p^{crit}, \qquad \varepsilon_f = \varepsilon_d + \varepsilon_{ccos}. \tag{19}$$

For pure shear, the pressure $p = 0$. With the prescribed monotonic loading, the Macaulay bracket term in the tearing parameter damage variable (1) reduces to the constant $\left(\frac{2}{3}\right)^4$ and the integral term reduces to the equivalent plastic strain scaled by this constant. The damage variable d is then given by

$$d = \frac{\left(\frac{2}{3}\right)^4 \bar{\varepsilon}^p}{t_p^{crit}} = \begin{cases} 0 & \text{for } \varepsilon_{12} \le \varepsilon_y \\ \left(\frac{2}{3}\right)^4 \left(\frac{2\sqrt{3}G\varepsilon_{12}-\sigma_y}{(3G+2H')t_p^{crit}}\right) & \text{for } \varepsilon_y < \varepsilon_{12} \le \varepsilon_d \\ 1 & \text{for } \varepsilon_{12} > \varepsilon_d \end{cases}. \tag{20}$$

Again, the yield surface radius is $r = \sqrt{2/3}\sigma$, except prior to yielding when it is $r = \sqrt{2/3}\sigma_y$.

The results of the analysis are shown in Figure 9 and Figure 10.

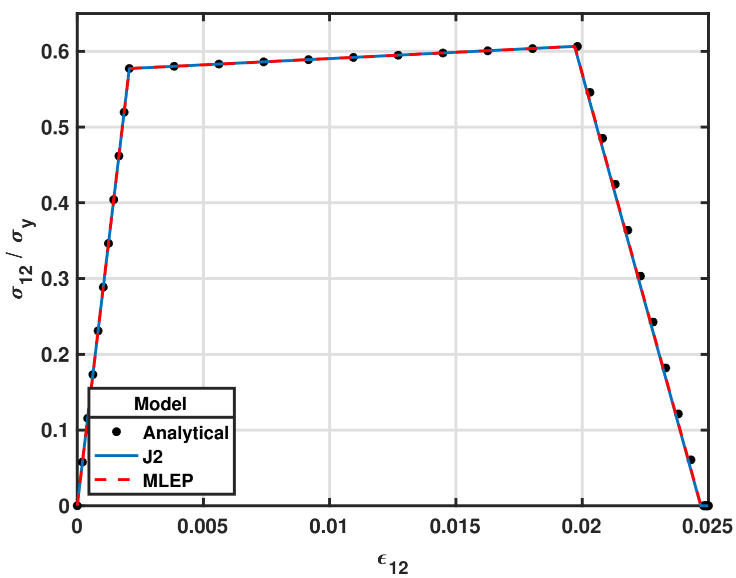

Figure 9. Stress-strain response for pure shear.

The stress-strain response and damage variable both match the analytical solution well for the J_2 plasticity model with modular failure and the MLEP model. Since there is no pressure in pure shear, the pressure decay algorithm is never active and there are no oscillations in the stress-strain response. The normal vector $\boldsymbol{n}_d$ in the direction of crack opening, aligned with the maximum principal stress direction, is not aligned with the coordinate axis as was the case with uniaxial tension, but rather was computed to be $\boldsymbol{n}_d = [-1/\sqrt{2}, -1/\sqrt{2}, 0]^T$. This normal vector is at 45° to the coordinate axes matching the analytical result.

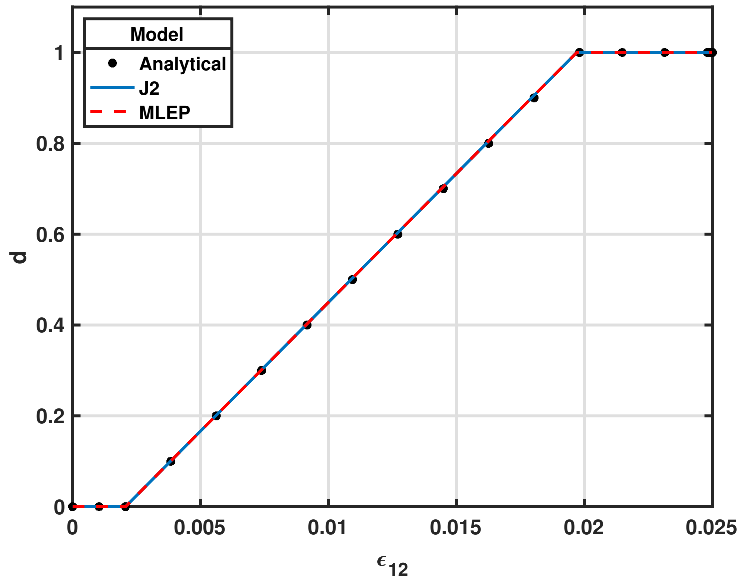

Figure 10. Tearing parameter damage variable for pure shear.

5 Future work

The J_2 plasticity model implementation is a first step towards adding the failure model as a modular failure option for any plasticity model. It was selected since both the J_2 plasticity model and the MLEP model use a von Mises yield surface. Many aspects of the failure propagation theory in Section 2.2 are completely general; however, the stress decay is achieved by scaling of the maximum yield stress. This limits the failure model to isotropic plasticity models with yield surfaces described in terms of a radius. For this model to be modular with any plasticity model, and anisotropic models in particular, the theory will need to be generalized. A brief list of future work to fully modularize the failure model is as follows:

(1) The current J_2 plasticity implementation is for a single element. For a single element the multilevel solver is not used. Implement the failure model for multi-element simulations, following the guide to interactions between LAMÉ material models and Sierra multilevel solver capabilities [5].

(2) Investigate the stability of constrained multi-element problems and revisit the pressure decay algorithm for potential improvements to eliminate spurious oscillations.

(3) Generalize the failure propagation method to anisotropic plasticity models and implement as a fully modularized failure model option for plasticity.

6 Conclusion

The tearing parameter criterion and failure propagation method currently used in the multilinear elastic-plastic constitutive model was added as a modular failure option for the J_2 plasticity model.

The implementation was verified against analytical solutions for both a uniaxial tension and a pure shear boundary-value problem. Possible improvements to, and necessary generalizations of, the failure method to extend it as a modular failure option for all plasticity models were highlighted.

7 Acknowledgements

The authors thank T. Shelton for helpful discussions on the original implementation of the MLEP material model and multilevel solver and W. Scherzinger for reviewing this work.

References

[1] LAMÉ Team. Library of advanced materials for engineering (LAMÉ) 4.56. Technical report, SAND2020-3408, Sandia National Laboratories, Albuquerque, New Mexico 87185 and Livermore, California 94550, March 2020.

[2] B. Lester and W. Scherzinger. Failure formulations in modular plasticity models. Technical report, SAND2019-9678 R, Sandia National Laboratories, Albuquerque, New Mexico 87185 and Livermore, California 94550, August 2019.

[3] B. Lester and W. Scherzinger. Modular growth and nucleation formulations in modular plasticity models. Technical report, SAND2020-7404 R, Sandia National Laboratories, Albuquerque, New Mexico 87185 and Livermore, California 94550, July 2020.

[4] G. Wellman. A simple approach to modeling ductile failure. Technical report, SAND2012-1343, Sandia National Laboratories, Albuquerque, New Mexico 87185 and Livermore, California 94550, June 2012.

[5] Solid Mechanics Team. Interactions between Lame material model and Sierra Solid Mechanics for material failure. Internal memo, Sandia National Laboratories, Albuquerque, New Mexico 87185 and Livermore, California 94550, December 2011.

Distribution:

MS-0840	E. Corona	1558
MS-0840	H. Fang	1558
MS-0840	B. Lester	1558
MS-0840	M. Neilsen	1558
MS-0840	W. Scherzinger	1558
MS-0845	T. Shelton	1542
MS-0845	J. Thomas	1542
MS-9042	G. Jose de Frias	8752
MS-9042	K. Karlson	8752
MS-9042	S. Nelson	8752
MS-9042	A. Stershic	8752
MS-9042	B. Talamini	8363